Growth Mechanism, Structural and Photoelectrochemical Study of Zinc Tellurium Thin Film

Kisan C. Rathod[1,*,], Kallappa R. Sanadi[2,], Pradip D. Kamble[3],
Ganesh S. Kamble[4,], Muddsar L. Gaur[5,] and Kalyanrao M. Garadkar[6]

[1]Department of Chemistry, The New College, Kolhapur-416012, India
[2]Department of Chemistry, Doodhsakhar Mahavidyalaya, Bidri, Kolhapur-416208, India
[3]Department of Physics, The New College, Kolhapur-416012, India
[4]Department of Engineering Chemistry, Kolhapur Institute of Technology's College of Engineering (Autonomous), Kolhapur-416234, India
[5]Department of Chemistry, C.B.Khedgi's Basaveshwar Science Raja Vijaysinh Commerce and Raja Jaysinh Arts College, Akkalkot, Solapur-413216, India
[6]Department of Chemistry, Shivaji University, Kolhapur-416004, India

*Corresponding author: Fax: +91 231 2621187, Tel: +91 231 2621180; E-mail: kishanchandurathod@gmail.com

Chalcogenides II-VI group of crystalline material zinc tellurium thin films have been synthesized by chemical bath deposition (CBD) method in which glass substrates have been used for deposition technique in presence of triethanolamine solution. The as-synthesized films were characterization by X-ray diffraction scanning electron microscopy (XRD), optical spectroscopy and thermoelectric techniques. The deposited material was orthorhombic in shape. The 2.01 eV is the optical band gap energy of the sample and the electrical conductivity of the thin film was originating in the order of 10^{-8} $(\Omega \, cm)^{-1}$, which showed n-type thermoelectrical conductivity. The solar cell can be represented as a n-ZnTe|NaI (0.1M) + I$_2$ (0.1M)|C$_{(graphite)}$. The solar efficiency of the cell was found to be 1.03%.

Keywords: Chemical bath deposition, Growth mechanism, Semiconductor, Photoelectrochemical cell.

INTRODUCTION

Now days, the development of semiconductor and photovoltaic solar cell technology was mainly contributed by thin film technique [1]. Over last two decades' semiconductors of II-VI compound play very important role in different fields due to its interesting properties. The semiconductor zinc is one of the most important semiconductors because of its optical and electrical properties. The direct band gap of zinc tellurium thin film varies from 1.7 eV to 2.6 eV. The energy gap for the semiconductor zinc telluride (ZnTe) depends on a group of factors, including preparation method, preparation temperature and the compounds used as sources for the zinc and tellurium elements and also have good optical absorption coefficient [2]. Hence, it is applied in optoelectronic and microelectronic devices such as X-ray imaging system [3], thin film transistors [4] and detectors [5]. Recently, the traditional ways of getting energy fails to fulfil the increasing demand and hence solar

energy is the need of time [6-8]. Thickness of thin film is ranging from nanometer to two microns, which possesses exclusive properties [9]. The crystal structure thickness is one of the main properties of thin film and other characterizing feature that are accessible in the material in its chemical bath deposition method [10].

Worldwide researchers are focusing on the designing of novel thin films with low cost. Such type of thin films is widely used in variety of applications such as electric devices in the form of resistors, transistor, capacitors and other is largely used in solar cell and photovoltaic cells [11]. The semiconductor ZnTe thin film is one of the most important semiconductors because of its optical and electrical properties [12]. In this synthesized method of zinc telluride thin films, the non-conducting glass substrate was used in aqueous alkaline medium. The deposition of ZnTe thin films have been passed by using numerous methods like thermal evaporation [13], electrodeposition [14], RF sputtering [15], electron beam evaporation [16],

molecular beam epitaxy (MBE) [17], hot-wall evaporation [18] and pulsed laser deposition (PLD) [19]. Numerous techniques were used in preparing this semiconductor, including thermal evaporation, chemical vapour deposition but until recently the chemical bath deposition technique we recently used for the preparation of ZnTe.

In this article, the synthesis of zinc telluride thin films by chemical bath deposition method is reported and their optical, structural, surface morphology, electrical properties and photo-electrical performance were also investigated.

EXPERIMENTAL

Synthesis of zinc tellurium thin film: All chemicals were used of AR grade for the synthesis of ZnTe thin films and double distilled water was used throughout the experiment. Zinc sulphate solution (0.2M, 10 mL) was taken in 250 mL beaker, 5 mL triethanolamines (TEA), 10 mL liquid ammonia, and 10 mL (0.2M) sodium teleurosulphate was further added in the reaction bath at room temperature, pH of the reaction mixture was found to be 10.5. In oil bath, beaker was kept and the glass substrate was stand vertically by holder which was specially designed. The reaction mixture were rotted with a speed of 65 ± 2 rpm. The temperature of the bath was increased slowly with 369 K. The slides were removed after 7 h 50 min and washed with deionized water several times, dried naturally and preserved in desiccator [20]. The deposition setup of the ZnTe thin film has been shown in Fig. 1.
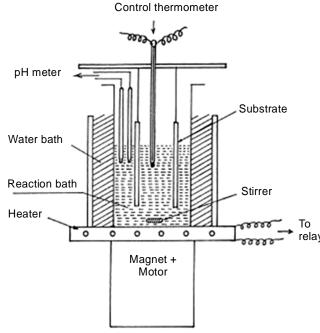

Fig. 1. Experimental deposition of the ZnTe thin films

Characterization: X-ray diffraction of zinc telluride thin films was measured out in the range of the diffraction angle 10-100º with CuKα1 radiation using Philips PW-1710 diffractometer ($\lambda = 1.54056$ Å). By using of 'dc' two-probe method, the electrical conductivity of zinc tellurium thin films was measured. For ohmic contact purpose, a rapid drying silver paste was

applied at the end of the film. The layer thickness of the film was calculated by weight difference method. In the wavelength range 400-1200 nm, the optical absorbance measurements were made by using a Hitachi-330 (Japan) UV-visible NIR, double beam spectrophotometer at room temperature, uncoated glass substrate placing in the reference beam made substrate correction. The morphology of the synthesized thin film was measured by A 250 MK-III StereoScon (USA) scanning electron microscope (SEM).

RESULTS AND DISCUSSION

Kinetics and growth mechanism: Zn^{2+} ions were complexed with TEA and Zn-TEA water soluble complex have been formed, thus concentrations of Zn^{2+} have been under constrained. The dissociation of sodiumtelenosulfate as well as Zn-TEA complex was takes place in alkaline medium. At low temperature kinetic energy is lower and avoids the precipitation [21]. Metastable complex delivered metal ions by thermal decomposition while sodium telenosulphate hydrolyzes in alkaline solution to yield Te^{2-} ions [22-24]. The kinetic expansion of film can be implied from the following mechanism:

$$Zn^{2+} + nTEA \longrightarrow [Zn(TEA)_n]^{2+} \tag{1}$$

$$Na_2TeSO_3 + OH^- \longrightarrow Na_2SO_4 + HTe^- \tag{2}$$

$$HTe^- + OH^- \longrightarrow H_2O + Te^{2-} \tag{3}$$

$$[Zn(TEA)_n]^{2+} + Te^{2-} \longrightarrow ZnTe + n(TEA) \tag{4}$$

The presence of generation period suggests that ion-by-ion growth mechanism. The graph of thickness against deposition temperature have been shown in Fig. 2a. Zinc tellurium thin films have been well deposited at 450 min with 0.276 µm thicknesses. The thickness was measured every 90 min and plotted against time as shown in Fig. 2b. Reaction mixture rotation speed was maintained at 65 ± 2 rpm to obtain constant deposition of zinc tellurium thin films. To obtained good thin film the optimum conditions like temperature and time were maintained at 369 K and 450 min, respectively.

X-Ray diffraction studies: X-ray diffraction studies of zinc tellurium thin films is shown in Fig. 3 'as deposited' and annealed thin films. Due to high crystalline, the XRD pattern of the 'annealed' sample shows high peak intensity. The observed
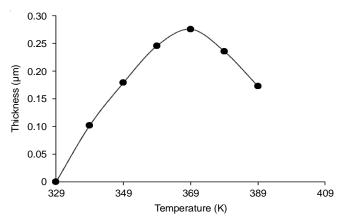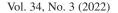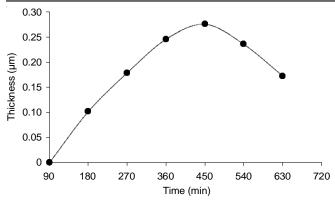

Fig. 2(a). Show deposition of thickness *vs.* temperature

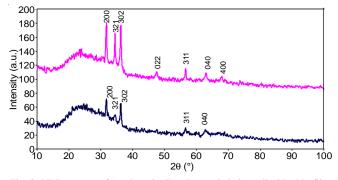Fig. 2(b). Show deposition of thickness *vs.* deposition time

Fig. 3. XRD pattern of 'as deposited' and annealed zinc telluride thin film

d-value correspond to 2.861 phase of zinc tellurium and are indexed according to orthorhombic structure (JCPDS File No. 822152). The XRD pattern shows the highest intensity reflection peak at *d* = 2.861 Å (200), along with (321), (302), (022), (311), (040) and (400) plane. The calculated lattice parameters are a = 4.7244 Å, b = 5.8796 Å, c = 5.010 Å, which are well agrees with obtained by Potlog *et al*. [25]. The orthorhombic phase was calculated by using following equation:

$$\frac{1}{d^2} = \frac{h^2}{a^2} + \frac{k^2}{b^2} + \frac{l^2}{c^2} \qquad (5)$$

By using Orthorhombic crystal structure, the lattice constant was calculated. The average grain size of the film was evaluated by using Scherrer's formula (eqn. 6):

$$D = \frac{K\lambda}{\beta\cos\theta} \qquad (6)$$

where D is crystallite size, λ is the wavelength used, β is the angular line width at half maximum intensity, θ is Bragg's diffraction angle and K is constant. The average crystallite

size of annealing zinc tellurium thin films at 373 K was found to be 18.6 nm (Table-1).

Morphological studies: A surface morphology of thin film was characterized by scanning electron microscopy (SEM), 250 MK III stereos can Cambridge, UK. The SEM images of the 'as deposited' thin film is shown in Fig. 4a. In SEM images, the well uniform grain size nanoparticles have been attached to the substrate. The distribution of spherical grains of almost similar size is observed (Fig. 4b). Most of the grains separated with each other. Cottrell's method [26] were used to determine the average grain size of ZnTe thin film.
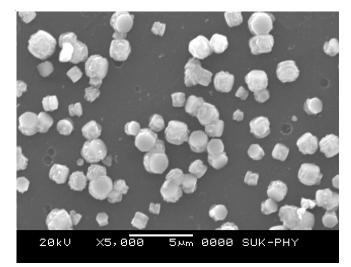

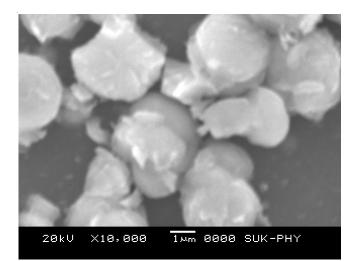Fig. 4(a). SEM micrograph as deposited ZnTe thin film

Fig. 4(b). SEM micrograph as annealed ZnTe thin film

TABLE-1
CRYSTALLOGRAPHIC PARAMETER OF ZINC TELLURIUM THIN FILM

Sample	d values (Å)		hkl planes	Grain size (nm) (XRD) (SEM)	Cell parameter, a, b, c (Å)
	ASTM	Observed			
ZnTe	2.869	2.861	200	18.6 18.3	a = 4.7244 b = 5.8796 c = 5.0100
	2.564	2.561	321		
	2.5050	2.499	302		
	1.9189	1.916	022		
	1.6244	1.620	311		
	1.4827	1.487	040		
	1.3647	1.367	400		

$$PL = \left(\frac{n}{2\pi r}\right)M \qquad (7)$$

where n is the total number of the intercept, M is the magnification, r is the radius of the circle. Knowing n, the average grain size of the deposited thin film as calculated. The average grain size for the deposited thin film is 18.3 nm.

Optical studies: At room temperature, the absorption spectrum of sample was measured in the wavelength range of 400-1200 nm. The absorption coefficients depend upon radiation energy as well as composition of thin films. It is probably due to increase in grain size leading to reduction in the density of grain boundary trapping centers and the change in the colour form white to gray white. The classical relation for near absorption edge in a semiconductor material is given by eqn. 8:

$$\alpha h\nu = A (h\nu - E_g)^n \qquad (8)$$

where hν, is the photon energy, E_g is the band gap, A is constant, and depending upon the temperature, photon energy, *etc*. For allowed direct transition n = ½ and allowed indirect transition n = 2. A plot of $(\alpha h\nu)^2$ *versus* hν is shown in Fig. 5. Extrapolation of the linear portion of the curve to $(\alpha h\nu)^2 = 0$ yields the optical band gap [20]. The observed straight-line establishes direct band gap is 2.01 eV [27,28].
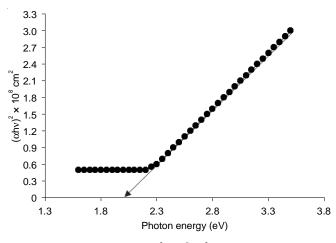

Fig. 5. Band gap energy $(\alpha h\nu)^2 \times 10^8$ cm² *vs.* photon energy (eV)

Electrical studies: The electrical characterization was carried out in the temperature range 300-525 K using two-probe method. The specific conductance was found to be into order of 10^{-8} $(\Omega\,cm)^{-1}$ at room temperature indicating that the conductivity behaviour of the film [29,30]. A plot of log (conductivity) *versus* inverse absolute temperature for the cooling and heating curve is shown in Fig. 6. The straight-line nature indicates the presence of only one type of conduction mechanism. According to the Arrhenius relation, the activation energy is calculated as follows:

$$\sigma = \sigma_o \exp\left(-\frac{E_a}{kT}\right) \qquad (9)$$

where E_a is the activation energy and other terms have their usual meaning. The activation energy was found to be of 0.370 eV. The electrical conductivity measurements show the n-type conduction mechanism of zinc telluride thin film.
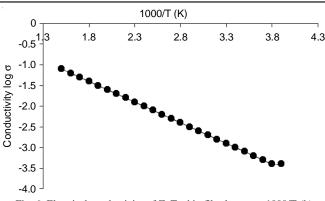

Fig. 6. Electrical conductivity of ZnTe thin film log σ *vs.* 1000/T (k)

Photoelectrochemical studies: Photovoltaic solar cell may operate over a wide range of voltages and currents. By applying the resistive load on an irradiated cell continuously from a short circuit to a very high value of open circuit, it is possible to determine the maximum power point ($P_m = V_m \times I_m$), that is the load for which the cell can deliver maximum electrical power. The power efficiency conversion factor can be calculated by using eqn. 10 [2,29]:

$$\eta_{max} = [V_{redox} - V_{fb}] \times \left(\frac{e}{E_g}\right) \qquad (10)$$

where V_{fb} is the flat band potential, V_{redox} is the electrolyte redox potential and E_g is the energy band gap. It is important to note that V_{oc} and η depends on V_{fb} and E_g. The low efficiency may be due high series resistance and interface states, which are responsible for the recombination mechanism. A photoelectrochemical solar cell zinc tellurium thin film can be represented as a n-ZnTe|NaI (0.1M) + I₂ (0.1M)|C$_{(graphite)}$. The photovoltaic power output characteristics for a cell, under enlightenment of 30 mW/cm is shown in Fig. 7. The short circuit current (I_{sc}) and open circuit voltage (V_{oc}) were found to be 376 µA and 500 mV, respectively. The power conversion of solar cell thin film efficiency was found to be 1.13%.
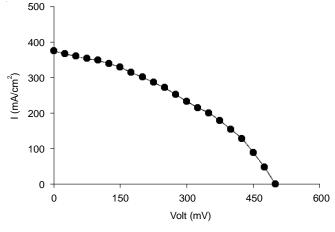

Fig. 7. Power output curves for ZnTe thin film solar cell

Conclusion

Binary zinc tellurium thin films have been deposited on to a glass substrate by using chemical bath deposition method.

The optical absorption studies showed zinc telluride sample have direct band gap of 2.01 eV. Current studies show that zinc-based II-VI compound semiconductors (*e.g.*, ZnS, ZnTe and ZnSe) have large band gap energy. Zn-X semiconductors can be applied to optoelectronic devices such as light emission diodes and photovoltaic solar cells. X-ray diffraction studies zinc telluride thin film are orthorhombic phase. The thermo-electrical properties of ZnTe show the n-type semiconducting nature of films. The material shows a promising photo-response when tested in I_2 electrolyte. The photoelectrochemical cell was found to be 1.03% efficiency.

ACKNOWLEDGEMENTS

CONFLICT OF INTEREST

The authors declare that there is no conflict of interests regarding the publication of this article.

REFERENCES

1. I.A. Younus, A.M. Ezzat and M.M. Uonis, *J. Nanocomposites*, **6**, 165 (2020);
    https://doi.org/10.1080/20550324.2020.1865712
2. H. Singh, M. Singh, J.S. Singh, B. Bansod, T. Singh, A. Thakur, M.F. Wani and J. Sharma, *J. Mater. Sci: Mater. Elect.*, **30**, 3504 (2019);
    https://doi.org/10.1007/s10854-018-00627-9
3. H. Bellakhder, A. Outzourhit and E.L. Ameziane, *Thin Solid Films*, **382**, 30 (2001);
    https://doi.org/10.1016/S0040-6090(00)01697-7
4. O. Toma, L. Ion, M. Girtan and S. Antohe, *Sol. Energy*, **108**, 51 (2014);
    https://doi.org/10.1016/j.solener.2014.06.031
5. H. Singh, P. Singh, A. Thakur, T. Singh and J. Sharma, *J. Mater. Sci. Semicond. Process.*, **75**, 276 (2018);
    https://doi.org/10.1016/j.mssp.2017.12.002
6. H. Singh, M. Singh, J. Singh, B.S. Bansod, T. Singh, A. Thakur, M.F. Wani and J. Sharma, *J. Mater. Sci. Mater. Electron.*, **30**, 3504 (2019);
    https://doi.org/10.1007/s10854-018-00627-9
7. M. Abbas, N.A. Shah, K. Jehangir, M. Fareed and A. Zaid, *Mater. Sci. Poland*, **36**, 364 (2018);
    https://doi.org/10.1515/msp-2018-0036
8. O.O. Abegund, E.T. Akinlabi, O.P. Oladijo, S. Akinlabi and A.U. Ude, *AIMS Mater. Sci.*, **6**, 174 (2019);
    https://doi.org/10.3934/matersci.2019.2.174
9. R.D. Gould, S. Kasap and A.K. Ray, Handbook of Electric and Photonic Materials, Springer International Publishing AG: Germany (2017).
10. A.M. Salem, T.M. Dahya and Y.A.El-Gendy, *Physica B*, **403**, 3027 (2008);
    https://doi.org/10.1016/j.physb.2008.03.005
11. Y.-T. Huang, S.R. Kavanagh, D.O. Scanlon, A. Walsh and R.L.Z. Hoye, *Nanotechnology*, **32**, 132004 (2021);
    https://doi.org/10.1088/1361-6528/abcf6d
12. W. Promnopas, T. Thongtem and S. Thongtem, *J. Nanomater.*, **2014**, 529629 (2014);
    https://doi.org/10.1155/2014/529629
13. K.M. Rehman, X. Liu, M. Riaz, Y. Yang, S. Feng, M.W. Khan, A. Ahmad, M. Shezad, Z. Wazir, Z.Ali, K.M. Batoog, S.F. Adil, M. Khan and E.H. Raslani, *Physica B*, **560**, 204 (2019);
    https://doi.org/10.1016/j.physb.2019.02.043
14. O.I. Olusola, M.L. Madugu, N.A. Abdul-Manaf and I.M. Dharmadasa, *Curr. Appl. Phys.*, **16**, 120 (2016);
    https://doi.org/10.1016/j.cap.2015.11.008
15. T. Kim, Y. Kim, I. Lee, D. Lee and H. Sohn, *Nanotechnology*, **30**, 13LT01 (2019);
    https://doi.org/10.1088/1361-6528/aafe13
16. T. Nakasu, W. Sun, M. Kobayashi and T. Asahi, *J. Cryst. Growth*, **468**, 635 (2017);
    https://doi.org/10.1016/j.jcrysgro.2016.11.035
17. T. Tanaka, H. Ohshita, K. Saito and Q. Guo, *Superlatt. Microstruct.*, **114**, 192 (2018);
    https://doi.org/10.1016/j.spmi.2017.12.034
18. A. Mondal, S. Chaudhuri and A. K. Pal, *Appl. Phys. A*, **43**, 81 (1987);
    https://doi.org/10.1007/BF00615211
19. B. Ghosh, D. Ghosh, S. Hussain, R. Bhar and A.K. Pal, *J. Alloys Compd.*, **541**, 104 (2012);
    https://doi.org/10.1016/j.jallcom.2012.06.063
20. P.P. Hankare, P.A. Chate, S.D. Delekar, M.R. Asabe and I.S. Mulla, *J. Phys. Chem. Solids*, **67**, 2310 (2006);
    https://doi.org/10.1016/j.jpcs.2006.05.001
21. C. Lincheneau, M. Oszajca, M. Amelia, M. Baroncini, S. Silvi, K. Szacilowski and A. Credi, *RSC Adv.*, **4**, 29848 (2014);
    https://doi.org/10.1039/C4RA03259D
22. D.C. Sharma, Y.K. Vijay, Y.K. Sharma and S. Srivastava, *Adv. Mater. Lett.*, **4**, 68 (2013);
    https://doi.org/10.5185/amlett.2013.icnano.118
23. S.S. Kale, R.S. Mane, H.M. Pathan, A.V. Shaikh, O.-S. Joo and S.-H. Han, *Appl. Surf. Sci.*, **253**, 4335 (2007);
    https://doi.org/10.1016/j.apsusc.2006.09.043
24. A.M. Aboraia, M. Ahmad, E.A. Abdel Wahab, H.S. Hassan and E.R. Shaaban, *Int. J. New Horiz. Phys.*, **2**, 11 (2015);
    https://doi.org/10.12785/ijnhp/020103
25. T. Potlog, N. Maticiuc, A. Mirzac, P. Dumitriu and D. Scortescu, *CAS 2012 (International Semiconductor Conference)*, **2**, 321 (2012);
    https://doi.org/10.1109/SMICND.2012.6400772
26. A. Cottrell, An Introducing to Metallurgy, Arnold: London, p. 173 (1975).
27. M.M. Uonis, B.M. Mustufa and A.M. Ezzat, *World J. Nano. Sci. Eng.*, **4**, 49518 (2014);
    https://doi.org/10.4236/wjnse.2014.43014
28. A.M. Ezzat, B.M. Mostafa and M.M. Younis, *Int. J. Sci. Technol.*, **9**, 72 (2014);
    https://doi.org/10.12816/0010141
29. Z. Li, J. Salfi, C. De Souza, P. Sun, S.V. Nair and H.E. Ruda, *Appl. Phys. Lett.*, **97**, 063510 (2010);
    https://doi.org/10.1063/1.3478555
30. V.B. Patil, D.S. Satraves, G.S. Shahane and L.P. Deshumkh, *Thin Solid Films*, **401**, 35 (2001);
    https://doi.org/10.1016/S0040-6090(01)01480-8